Supporting Information

Thiahelicene-based inherently chiral films for enantioselective electroanalysis

Serena Arnaboldi[*], *Silvia Cauteruccio*[*], *Sara Grecchi, Tiziana Benincori, Massimo Marcaccio, Alessio Orbelli Biroli, Giovanna Longhi, Emanuela Licandro, Patrizia Romana Mussini*[*]

SI.1.First electrooligomerization cycles of 7-TH monomer in DCM and ACN

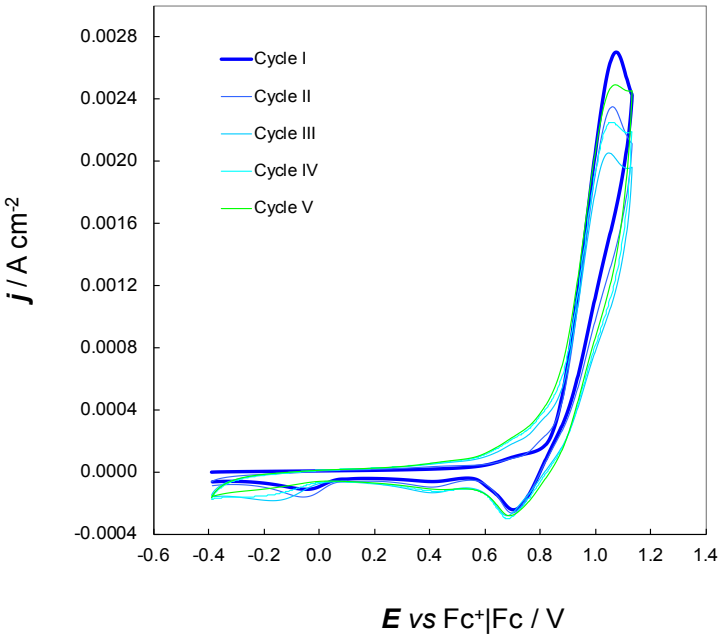

Figure SI.1a. Electrooligomerization (five cycles) of **7-TH** monomer on GC electrode at 0.2 V/s in DCM + $TBAPF_6$ 0.1 M

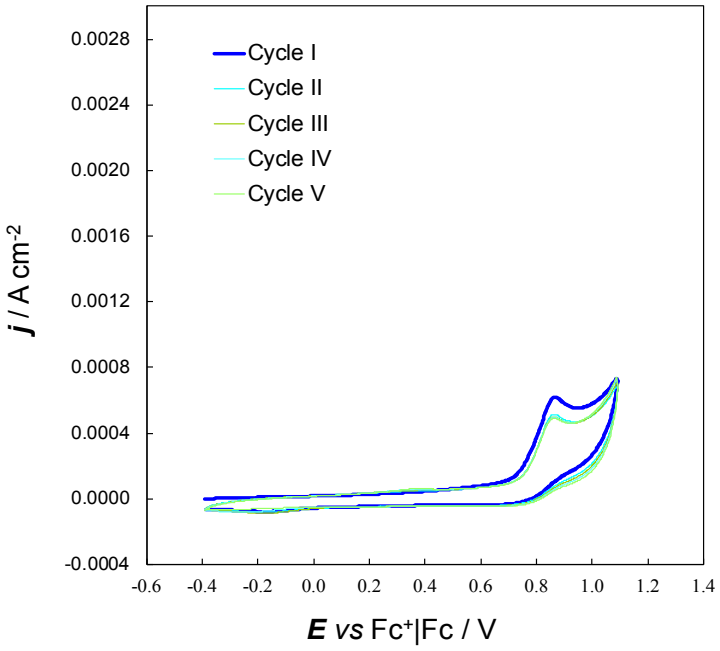

Figure SI.1b. Electrooligomerization (five cycles) of **7-TH** monomer on GC electrode at 0.2 V/s in ACN + $TBAPF_6$ 0.1 M

SI.2 Estimated average thickness and roughness of electrodeposited oligomer layers from profilometry measurements

Tab. SI.2.1 7-TH in DCM

deposition cycles	*thickness (d, µm)*	*roughness (R_a-R_q, µm)*
50	0.3	0.1-015
100	2.2	0.2-0.3
144	3.5	0.2-0.3

Ra: average roughness; Rq: RMS roughness

Tab. SI.2.2 BT_2T_4 in DCM

deposition cycles	*thickness (d, nm)*	*roughness (R_a-R_q, µm)*
36	n.d.	16-21
77	n.d.	45-86
100	50	44-62
144	120	48-61

n.d.= not detectable

Tab. SI.2.3 BT_2T_4 IN ACN

deposition cycles	*thickness (d, µm)*	*roughness (R_a-R_q, µm)*
36	0.45	0.31-0.45
77	0.90.	0.45-0.57
108	1.80	0.52-0.63

SI.3. MALDI spectra of electrodeposited films, and related temptative assumptions about oligomer structures

MALDI mass spectra were recorded with a MALDI-TOF/TOF Autoflex III-Bruker Daltonics, using dithranol as matrix.

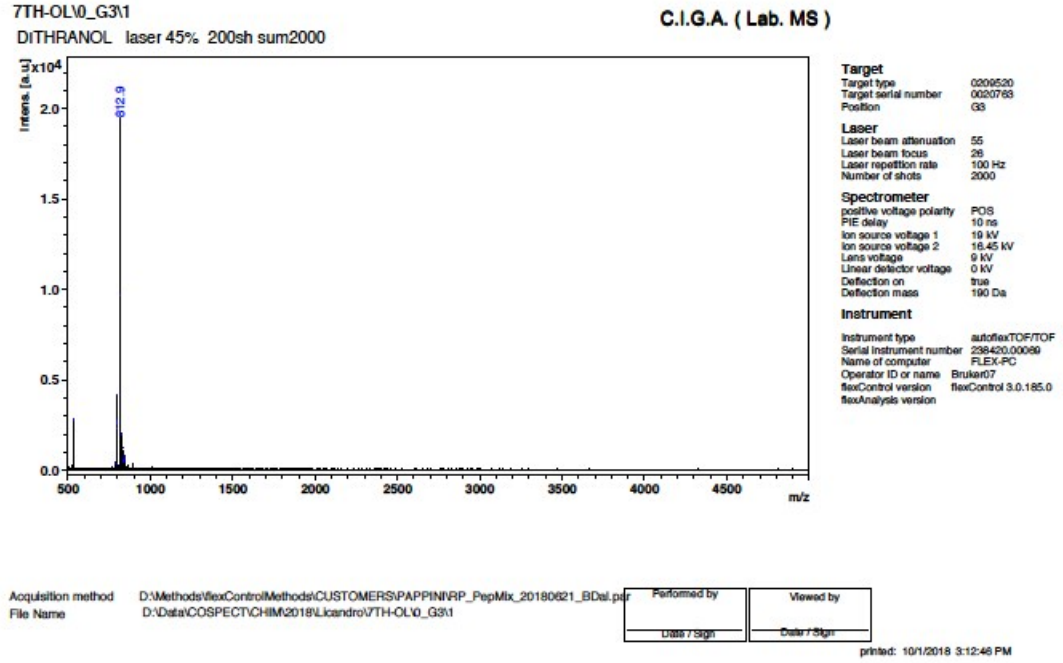

Figure SI.3.1 Experimental MALDI spectrum of the mixture resulting from the electrooxidation of (±)-**7TH** on ITO electrode.

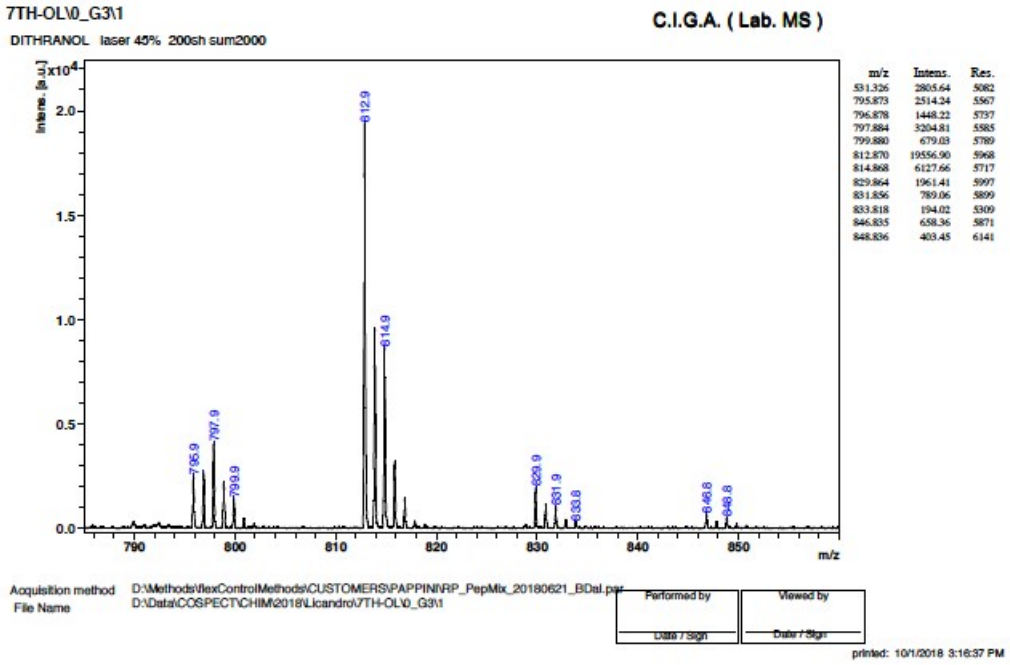

Figure SI.3.2. Experimental MALDI spectrum of the mixture resulting from the electrooxidation of (±)-**7TH** on ITO electrode in the range of m/z = 785□860.

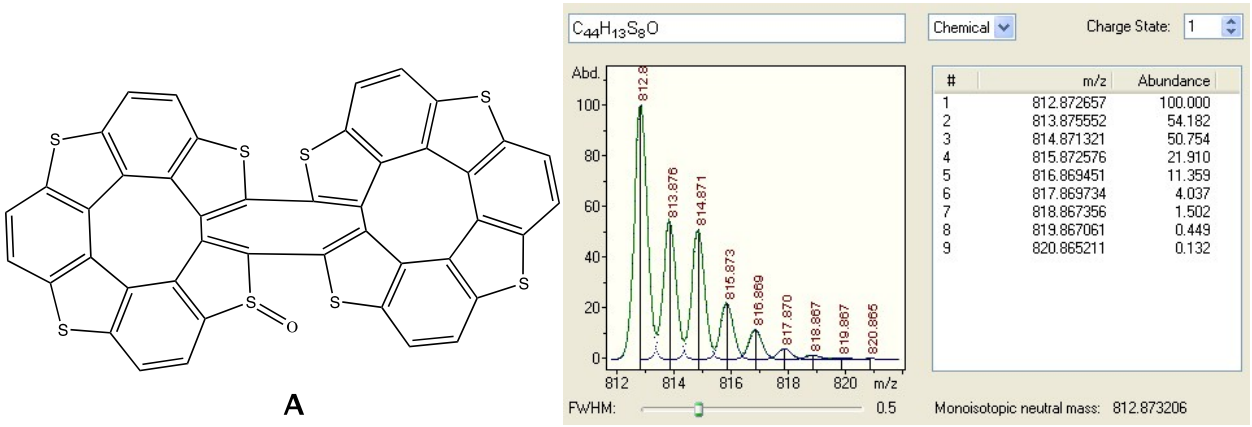

Figure SI.3.3 Formula and calculated MALDI mass spectrum for the main compound at m/z 812.9.

The comparison between experimental and calculated MALDI mass spectrum suggests a molecular formula of $C_{44}H_{13}S_8O$ as protonated adduct. Taking into account the considerations on AFM studies and the possibility of oxidation processes during the electrooxidation, we could assign at this molecular formula the structure **A**.

On the other hand, the signals related at m/z values ranging from 795.9 to 799.9 could be assigned at a mixture of the structures **B** and **C** with a molecular formula of $C_{44}H_{12}S_8$ and $C_{44}H_{14}S_8$, respectively. For these structure, no protonated adduct seems to be present, presumably due to the absence of the oxygen atom that can be easy protonated by the matrix.

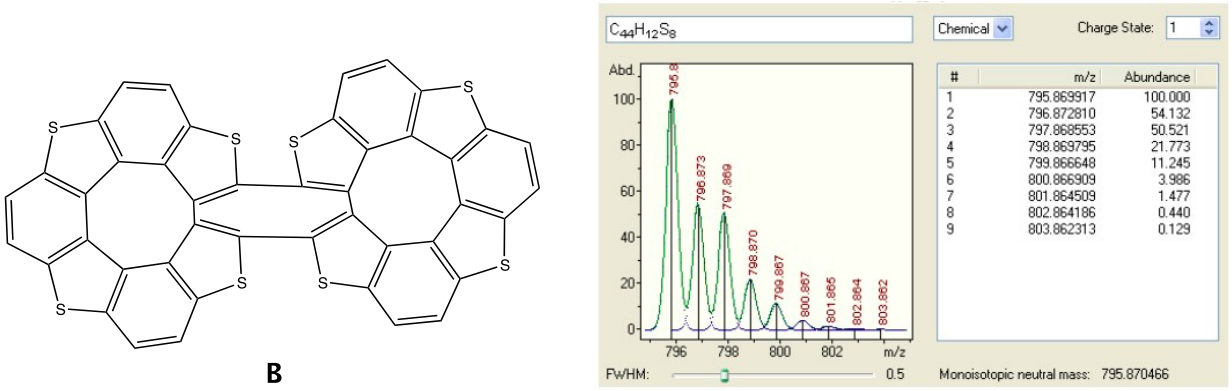

Figure SI.3.4. Calculated MALDI mass spectra for structure **B**

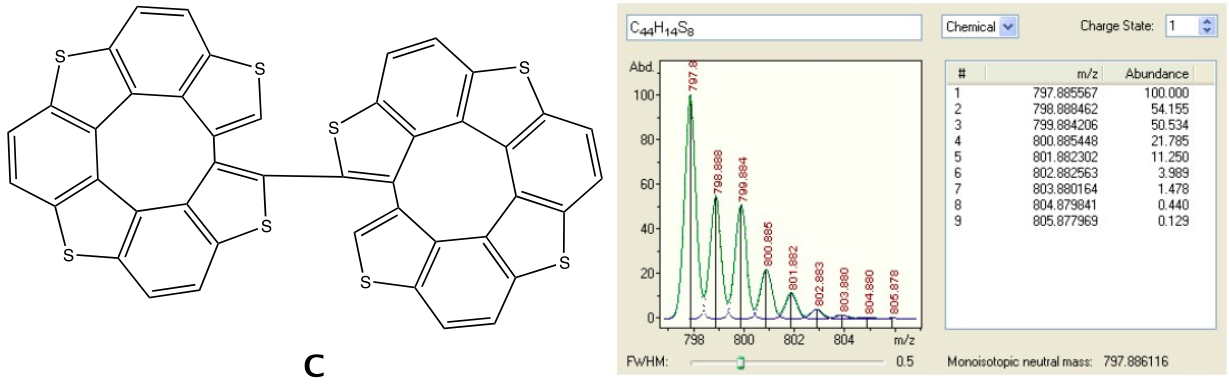

Figure SI.3.5. Calculated MALDI mass spectra for structure **C**.

SI.4. DFT calculations

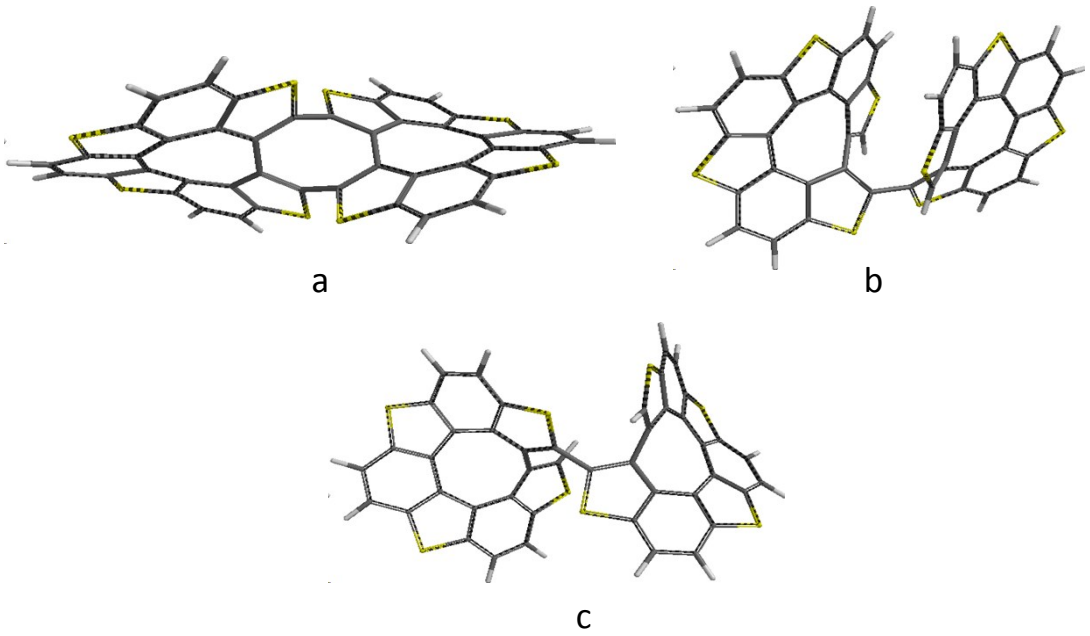

Figure SI.4.1. Optimized molecular structures for dimers of **7-TH** at DFT B3LYP/6-31G* level. Top: two structures possibly resulting from homochiral coupling of two *P*-monomers (a: closed dimer, b: open dimer). Bottom: a structure possibly resulting from heterochiral coupling of one P and one M enantiomer (open dimer).

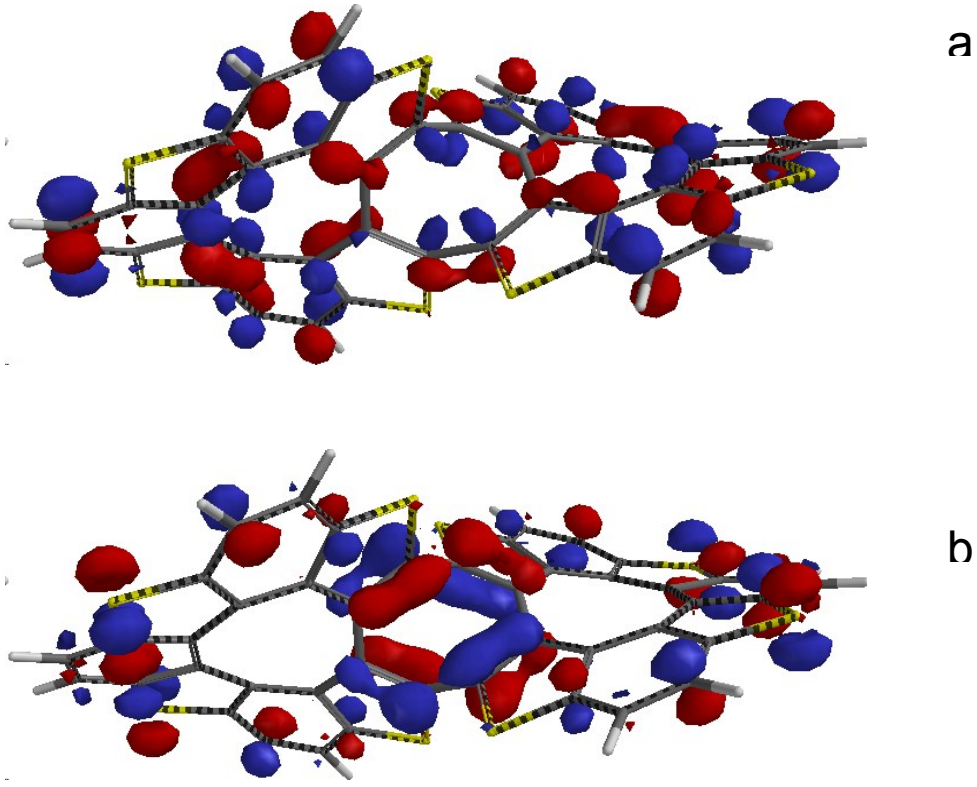

Figure SI.4.2 Frontier Molecular Orbital surfaces for the optimized structure of **7-TH** discoid dimer at DFT B3LYP/6-31G* level with two "intrahelicene" C-C bonds between the β positions of each **7-TH** moiety terminals plus two "interhelicene" ones between the α positions of facing **7-TH** units, as shown in Figure 5a. (a) LUMO energy E= -1.90 eV; (b) HOMO energy E= -5.53 eV.

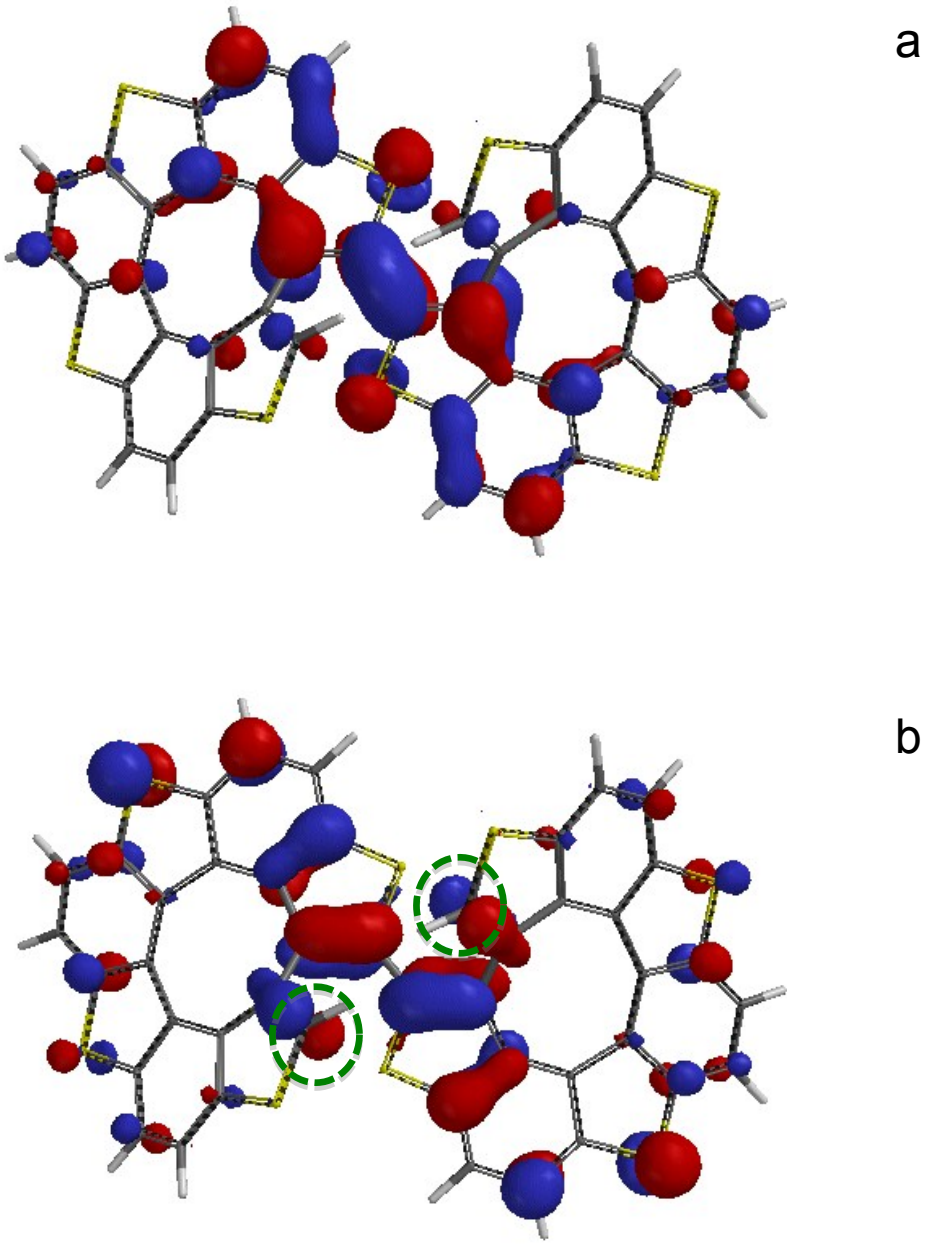

Figure SI.4.3 Molecular Orbital Surfaces for the optimized structure of **7-TH** homochiral open dimer (structure b in Figure SI.4.1) at DFT B3LYP/6-31G* level with a *trans*-conformation of the two monomers. (a) LUMO with E= -2.18 eV; (b) HOMO, E= -5.27 eV. The dashed green circles indicate the two C atoms of the thiophene moieties that have a high contribution to the HOMO and that can undergo coupling upon oxidation to give the discoid structure of the closed homochiral dimer (structure a in Figure 4 and Figure SI.4.1).